Load optimised piezoelectric generator for powering battery-less TPMS

D. Blažević*[a], E. Kamenar [a], S. Zelenika [a]

[a] University of Rijeka, Faculty of Engineering and Centre for Micro and Nano Sciences and Technologies, Rijeka, Croatia

ABSTRACT

The design of a piezoelectric device aimed at harvesting the kinetic energy of random vibrations on a vehicle's wheel is presented. The harvester is optimised for powering a Tire Pressure Monitoring System (TPMS). On-road experiments are performed in order to measure the frequencies and amplitudes of wheels' vibrations. It is hence determined that the highest amplitudes occur in an unperiodic manner. Initial tests of the battery-less TPMS are performed in laboratory conditions where tuning and system set-up optimization is achieved. The energy obtained from the piezoelectric bimorph is managed by employing the control electronics which converts AC voltage to DC and conditions the output voltage to make it compatible with the load (i.e. sensor electronics and transmitter). The control electronics also manages the sleep/measure/transmit cycles so that the harvested energy is efficiently used. The system is finally tested in real on-road conditions successfully powering the pressure sensor and transmitting the data to a receiver in the car cockpit.

Keywords: energy harvesting, tyre pressure monitoring, design optimisation, power requirements, on-road assessment

1. INTRODUCTION

Energy harvesting is the process of collecting low level ambient energy and its conversion into electric power via devices based on photovoltaics, thermoelectrics, radio frequency (RF) and radiation sources, electromagnetic conversion or harvesting of kinetic energy (e.g. fluid flow or vibrations) [1]. Kinetic energy harvesting is developing rapidly in the last decade with numerous new proposed applications and design solutions which overcome the current limitations of such systems, especially by widening their operating frequency bandwidth [2]. Harvesting the kinetic energy of vibrations can be performed by using piezoelectric, electromagnetic or capacitive phenomena. The harvesting via piezoelectric bimorph cantilevers so as to generate electric power is particularly advantageous due to design simplicity, miniaturization potential as well as the linearity of the mechanical behaviour and of the electromechanical coupling [3]. A bimorph cantilever covered with piezoelectric material with a tip mass at its free end is thus placed in a vibrating environment and excited at cantilever's fixation. As the cantilever bends, charge is accumulated on the surface of the piezoelectric material and conducted to a load via copper electrodes. In this manner AC current is produced and mechanical bending energy is transformed into electric energy [3, 4].

Taking into account that power consumption of digital processors halves each 18 months (so called Gene's Law), autonomous low power electronic devices powered via energy harvesting become thus feasible. Special interest in energy harvesters is therefore foreseen in the development of autonomous sensor nodes in pervasive wireless networks [5]. Conventional wireless sensor nodes have, in fact, a limited life span restricted by the respective batteries which have to be periodically changed. This limits the range of employment of wireless networks especially if the nodes are to be placed in remote or dangerous environments. By using energy harvesting devices, these obstacles are easily avoided. Other potential applications of wireless systems based on energy harvesting devices include healthcare and body monitoring sensors, structural health monitoring, transportation, machine tool monitors, communication systems, unmanned air vehicles and aerospace, robotics, MEMS devices, everyday gadgets and toys and several other sectors [6].

Tire pressure monitoring has been proven to be extremely important when considering passenger safety. Correctly regulated tire pressures could save lives and drastically improve tire lifetime. In fact, 9% of traffic accidents are caused by improper tire inflation while an underinflation in the range of 0.2 bars increases fuel consumption by 2% and reduces

* dablazev@riteh.hr; phone + 385 – (0)51 - 651585; fax +385 – (0)51 - 651416; www.riteh.uniri.hr & www.cmnzt.uniri.hr

tire lifetime by 25% [7]. Correctly regulated tire pressures ensure a stronger grip and reduce tire slippage. Tire pressure monitoring systems (TPMS) are already being therefore installed on new vehicles but most of them are still powered by batteries. In turn, battery lifetime predictions are in the range of 5-7 years, while car lifetimes are estimated is in the range of 13 years. Taking into consideration the TREAD act passed in the USA in 2001 (active from 2007), and a similar act passed in the EU in 2008 (effective from 2013), which mandate the installation of TPMS in all new vehicles, a total of 10 batteries (and, due to hermetic enclosure, whole TPMS devices) are to be disposed into the environment in a single car lifetime. Knowing that the USA produces 16 million new vehicles annually, this represents 80 million batteries which are to be disposed of in the next 5 years!

Figure 1. Battery-less TPMS concept: 1) piezoelectric harvester, fixation and conditioning electronics, 2) tire pressure sensor and transmitter electronics, 3) standard Schrader valve

In this work an overview of the technological project aimed at developing a battery-less TPMS prototype consisting of a pressure sensor with a wireless module mounted at the tire valve and a central receiver unit located in the car cockpit, is presented. The sensor and the wireless module are powered by an energy harvesting mechanism consisting of a bimorph piezoelectric cantilever, a custom-developed cantilever fixation and the power conditioning electronics (Figure 1). Prior to the design optimization phase, an analysis of wheel vibrations is performed in different driving conditions to determine the main frequency bandwidths and vibration amplitude levels. Laboratory and 'on-car' experimental set-ups are hence developed and tested.

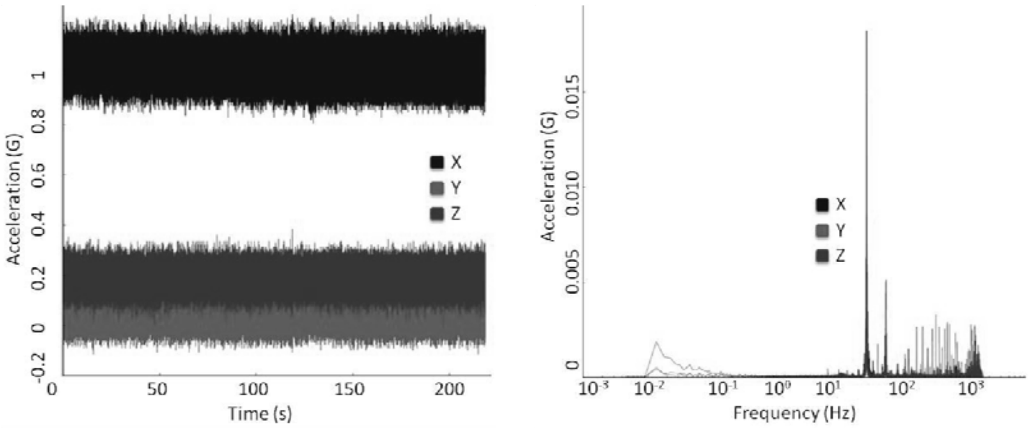

Figure 2. Amplitude/time histogram and FFT for a parked car with running engine

2. ON-ROAD VIBRATION MEASUREMENTS AND ANALYSIS

Vibrations as an energy source are found in abundance in the surrounding of motor vehicles such as cars, motorcycles, trucks etc. Part of these vibrations occurs as a result of the interaction between the vehicle wheels and road surface irregularities. On the other hand, vibration energy harvesting devices are often designed to work at a specific excitation frequency so as to maximize energy conversion output at the first eigenfrequency of the device.

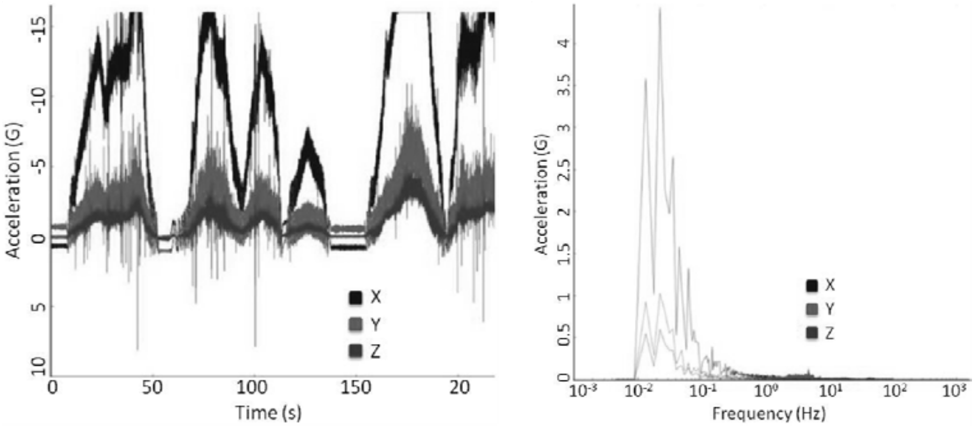

Figure 3. Amplitude/time histogram and FFT for city driving conditions at 40 km/h

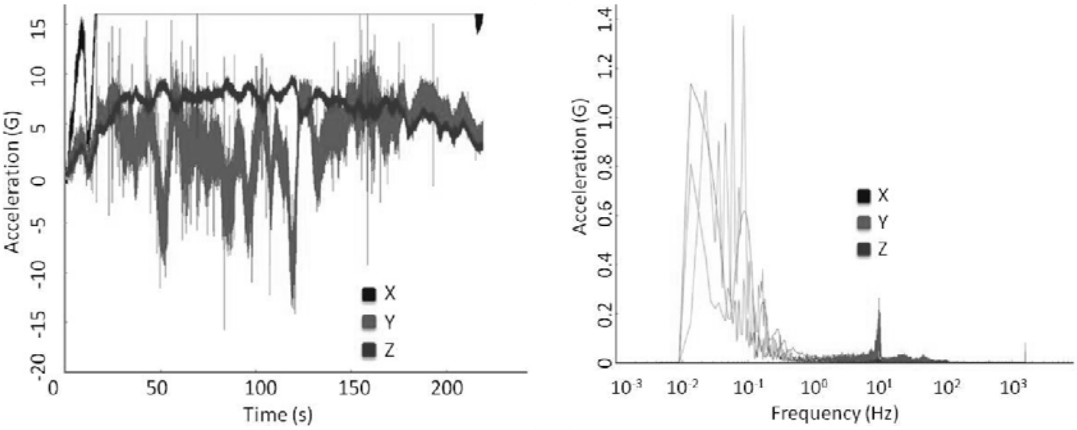

Figure 4. Amplitude/time histogram and FFT for open road driving conditions at 70 km/h

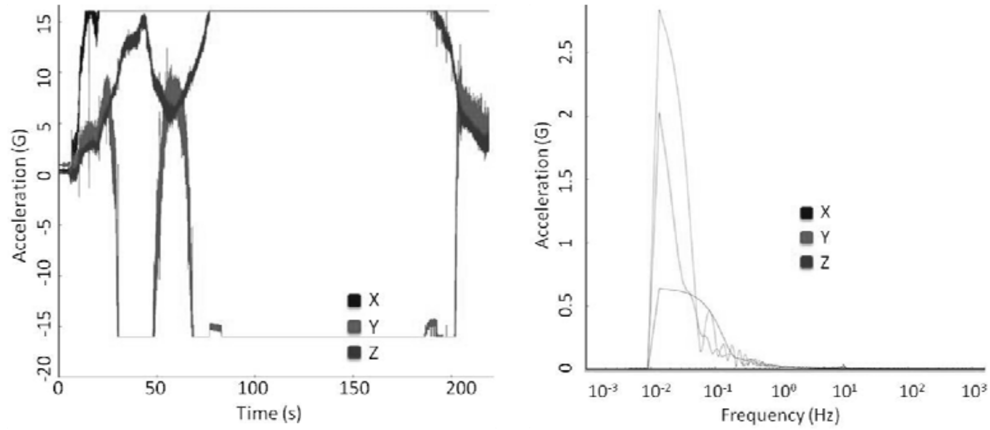

Figure 5. Amplitude/time histogram and FFT for highway driving conditions at 120 km/h

In order to investigate the frequencies and amplitudes of vibrations present on a car wheel in different driving conditions, series of experiments are performed. To measure the desired values on a rotating wheel, a wireless vibration logging device – Slam Stick Vibration Recorder triple axis accelerometer [8] is used. This device can measure vibration amplitudes of up to 16 G within frequency bandwidths from 10 Hz up to 3.2 kHz. The maximum measurement interval is set to 3.6 minutes. The obtained results are shown in Figures 2-5.

Experiments aimed at the determination of vibration frequencies and amplitudes are performed in 4 different conditions: a) parked car with running engine, b) city driving conditions while maintaining the speed at v = 40 km/h, c) open road conditions at the speed of v = 70 km/h and d) highway conditions while maintaining the speed at v = 120 km/h. In each condition, a series of four experimental runs is undertaken. While in parked mode, the vibration amplitudes are expectedly very low, with the largest amplitudes resulting from the gravity and from engine vibration effects at around 30 Hz (Figure 2). The measurements on city roads result in high amplitudes (over 16 G on the x axis) at very low frequencies (10^{-2} Hz) with some periodic amplitudes noticeable around 15 Hz and 45 Hz (Figure 3). These results can be accounted to bumps on the road and higher achieved driving speeds. While the car is standing still at a red light or in a traffic jam, the amplitudes drop to 0 G or 1 G depending on the orientation of the vibration logger axis (1 G as a result of gravity). Similar results occur while performing measurements in open road (Figure 4) and highway conditions (Figure 5), the only difference being in the magnitude of the amplitudes which rise beyond the measurement range of the vibration logger. These measurements proved hence the initial expectations of having very high amplitudes occurring in an unperiodic manner, thus not limiting the TPMS design to a specific resonant frequency of the cantilever [6].

3. SYSTEM ARCHITECTURE

In this section, the main elements of the battery-less TPMS are described. The system consists of the piezoelectric bimorph harvester, the power conditioning electronics and the sensor electronics with the transmitter. The measured tire pressure value is transmitted to the receiver in the car cockpit (Figure 6).

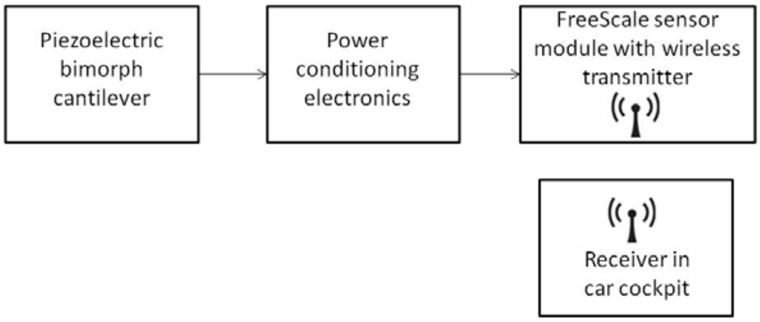

Figure 6. Main battery-less TMPS components

Table 1. Piezoelectric bimorph specifications

Model	Length (mm)	Width (mm)	Thickness (mm)	Free length (mm)	Total deflection (mm)	Blocking force (N)	Resonant frequency (Hz)	Capacitance (pF)
40-2020	40	20	0,70	30	> 1,1	> 0,60	170	120.000

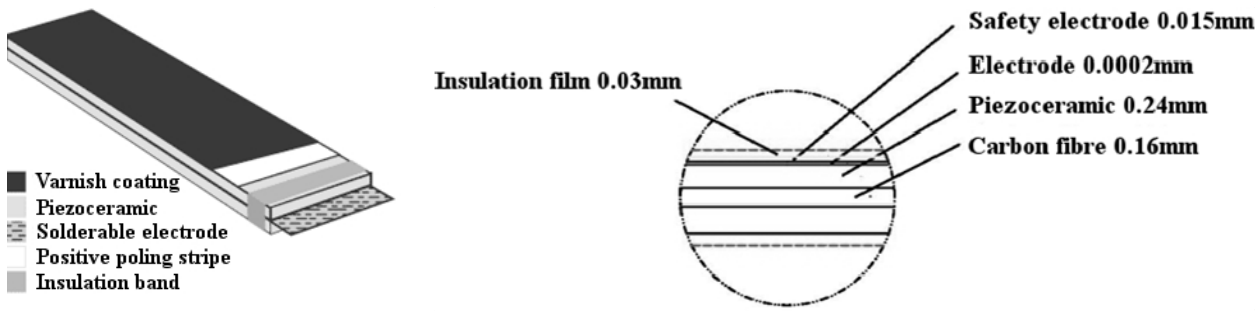

Figure 7. Piezoelectric bimorph (courtesy of APC International)

3.1 Piezoelectric harvester

The energy harvesting mechanism is based on employing piezoelectric bimorph cantilevers in the bending mode to convert mechanical vibration energy into low level AC electric energy. Conventional piezoelectric bimorphs generally consist of five laminated layers: two poled piezoceramic layers, two electrodes and a middle metallic substrate layer.

However, most of the commercially available benders have more than five layers, i.e. also additional bonding layers, protective layers, etc. The cross section of the bimorphs used in this work is shown in Figure 7, while the respective main specifications are given in Table 1 [9].

3.2 Power conditioning electronics

Due to the effects of bending of the piezoelectric bimorph caused by the kinetic energy of vibrations, a varying AC voltage is generated at the output of the bimorph. The resulting energy must be managed appropriately to be used for powering an electrical system such as the tire pressure sensor electronics.

The LTC3588-1 Linear technology chip is hence used. The chip is an ultralow quiescent current integrated circuit designed for powering low power consumption electronics and sensors and it is optimized for energy sources with high output impedances, such as piezoelectric cantilevers. The input voltage range for this integrated circuit can be in the range from V_{IN} = 2.7 V to 20 V, while the used piezoelectric cantilevers can generate voltages larger than 20 V. If the piezoelectric element generates excessive voltages, an input protective shunt, embedded in the chip and set to 20 V, is activated and voltage is clipped. Moreover, the chip is designed to interface directly to a piezoelectric power source, rectify the voltage waveform via a full-wave bridge and store the harvested energy on an external capacitor, as well as to maintain a regulated output voltage. When the voltage of the external input capacitor is higher than a threshold determined via a pin selection, the energy from the capacitor is delivered to the load [10]. A 3.3 V output voltage is used in the final system set-up.

When the energy on the input capacitor is high enough to power the load, it is transferred to the output capacitor. The two capacitors should be optimized based on the load connected to the harvester (see below). When voltage is brought into the system, any excess energy is stored on the input capacitor and its voltage increases. While energy storage at the input utilizes high voltage, the load current is limited to the value that the buck converter can supply. In the herein considered case, high powers must be supplied in short periods of time; the output capacitor is hence sized to support a larger current for a short time [10]. The used optimization procedure and the selection of the respective passive elements are described in section 4 below.

3.3 Sensor electronics with transmitter

The used FreeScale MPXY8300 kit consists of a sensor module with an embedded wireless transmitter and a receiver. Several sensors are embedded in the respective module: a temperature sensor, a dual-axis accelerometer and a capacitive pressure sensor. The module also encompasses a microcontroller and an RF transmitter. Freescale’s MPXY8300 tire pressure module’s chipset main characteristics are given in Table 2 [11].

Table 2. Specifications of the Freescale MPXY8300 sensor module with wireless transmitter

Microcontroller	RF Transmitter	Sensors
8-bit S08 MCU	315/434 PLL-based RF transmitter	X- and Z- accelerometers
16 KB flash		Pressure and temperature sensors
512B RAM		±10 kPa pressure sensor accuracy (in 100 – 800 kPa pressure range, 0 to 70˚C)
2-channel, 16-bit timer/pulse width modulator	ASK and FSK modulation	Power management filter designed for media protection
8-channel, 10-bit analog-to-digital converter		Integrated filter designed for media protection
Serial peripheral interface		SOIC 20 WB package
		-40˚C to +125˚C

4. LABORATORY EXPERIMENTS

4.1 Power requirements of the sensor electronics and transmitter

As mentioned above, the input and output capacitors should be sized based on load requirements. In this case the sizing should thus allow successfully driving the sensor electronics and the transmitter. The input capacitor should hence be able to store enough energy to power the load for the required time. In order to optimize the harvester for the FreeScale module, measurements of the power consumption are conducted. A laboratory UTP3704 DC power supply [12] is used to power the sensor module, while an Agilent InfiniiVision DXO-X 2012A oscilloscope [13] is used to determine the power consumption of the module. Since the oscilloscope is not suitable for measuring power consumption or electric current directly, the power requirements of the electronics are determined by measuring the voltage on a known resistor connected in series with the harvester output pins and the sensor module. Two resistance values (10 and 22 Ω) are used in order to verify the results; small resistance values are selected so as to minimize power dissipation and assure unobstructed operation of the system. The *RMS* voltages on the resistors (V_{R_RMS}) in a typical data transmission time period are shown in Figure 8.

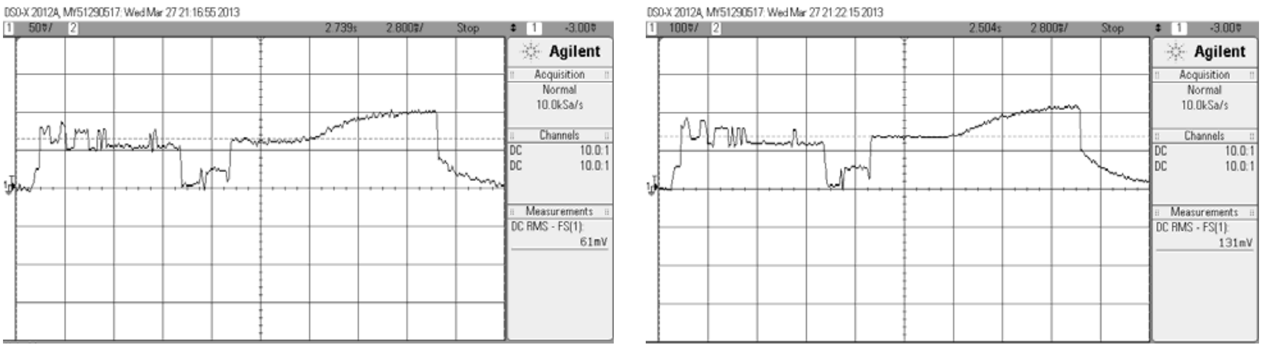

Figure 8: Measurements of the *RMS* voltage on the resistor with R = 10 Ω (left) and with R = 22 Ω (right)

For the duration t_{TPMS} of data transmission, the current I_{TPMS} in the serial circuit can be determined by using Ohm's law:

$$I_{TPMS} = \frac{V_{R\_RMS}}{R} \tag{1}$$

Considering the measured voltages V_{R_RMS}, in the case when the 10 Ω resistor is used the resulting current will thus be:

$$I_{TPMS} = \frac{61\,\mathrm{mV}}{10} = 6.1\,\mathrm{mA} \tag{2}$$

while in the case of the 22 Ω resistor I_{TPMS} is:

$$I_{TPMS} = \frac{131\,\mathrm{mV}}{22} = 5.95\,\mathrm{mA} \tag{3}$$

Therefore, an average value I_{TPMS} = 6 mA is adopted. Neglecting the small voltage drop on the resistor, the output voltage from the harvester delivered to the load is approximately V_{TPMS} = 3.3 V. The power delivered to the load in the considered transmission time period can hence be calculated as:

$$P_{TPMS}(t_{TPMS}) = I_{TPMS}(t_{TPMS}) \cdot V_{TPMS} = 6\,\mathrm{mA} \cdot 3.3\,\mathrm{V} \approx 20\,\mathrm{mW} \tag{4}$$

It should be mentioned here that the calculated power consumption is for short time periods only, i.e. for the time necessary for the transmission of the data to occur.

4.2 Selection of power conditioning electronics' passive elements

Knowing the power requirements of the load (i.e. the sensor electronics and transmitter), the passive elements of the power conditioning electronics are optimized next. The value of the input capacitance C_{IN} is thus determined from the expression for the needed power P_{LOAD} in the required time interval t_{LOAD} [10]:

$$P_{LOAD}\, t_{LOAD} = \frac{1}{2} \cdot \eta \cdot C_{IN} \cdot \left(V_{IN}{}^{2} - V_{UVLOFALLING}{}^{2}\right) \tag{5}$$

whence:

$$C_{IN} = \frac{2 \cdot P_{LOAD}\ t_{LOAD}}{\eta \cdot \left(V_{IN}^{\ 2} - V_{UVLOFALLING}^{\ \ 2}\right)} \tag{6}$$

where V_{IN} is the input voltage when the buck begins to switch, $V_{UVLOFALLING}$ is the threshold undervoltage lockout voltage while V_{IN} is falling and η is the average efficiency of the buck converter in the input range. The value of V_{IN} depends on the vibrations of the cantilever and it cannot be determined exactly; an average value between the extremes V_{INMIN} = 10 V and V_{INMAX} = 20 V is thus taken, i.e. V_{IN} = 15 V. V_{INMIN} is experimentally determined in laboratory conditions, whereas V_{INMAX} is limited to 20 V by the internal shunt embedded in the LTC3588-1 power conditioning electronics chip. For the 3.3 V output voltage selection, the typical value for $V_{UVLOFALLING}$ is 3.67 V. The average efficiency of the buck converter is a function of the input voltage (V_{IN}), the load current (in this case I_{TPMS}) and the inductance of the inductor (L); for the used system set-up, it is estimated from the data reported in [10].

Since the value $P_{TPMS}(t_{TPMS})$ is determined for the duration of data transmission, i.e. in the time period in which the TPMS module is powered, it can be equated to the left side of equation (5):

$$P_{TPMS}\ (t_{TPMS}) = P_{LOAD}\, t_{LOAD} \tag{7}$$

The optimal value of C_{IN} can finally be calculated from equations (6) and (7) as:

$$C_{IN} = \frac{2 \cdot 20 \cdot 10^{-3}}{0.8 \cdot \left(15^2 - 3.67^2\right)} = 2.36 \cdot 10^{-4} = 236\ \mu\text{F} \tag{8}$$

The closest standard value C_{IN} = 220 µF is finally adopted.

The value of the capacitance C_{OUT} is determined experimentally. A capacitor with a capacitance smaller than 10 µF is not recommended since the ripple of the output voltage could increase to an undesirable level. On the other hand, the sleep time decreases as the load current increases and/or as the output capacitance decreases. In the considered case an optimal value C_{OUT} = 47µF is thus determined.

A 1 µF capacitor is additionally connected between V_{IN} and *CAP* where it serves as a gate drive for the buck PMOS switch. A 4.7 µF capacitor is connected between V_{IN2} and *GND* and it is intended as a gate drive for the buck NMOS switch. Although in [10] a recommended value for the inductance of the inductor is L = 10 µH, a value of 20 µH is adopted to increase slightly the efficiency of the buck converter.

The hence obtained architecture of the battery-less TPMS with all passive elements and their values is given in Figure 9.

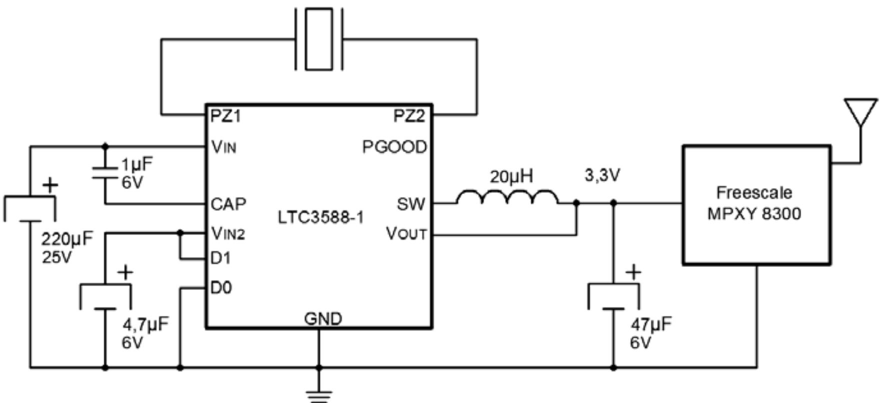

Figure 9. Architecture of the battery-less TPMS

4.3 Measurement of power delivered from final system set-up to the load

The power delivered to the load is measured next in the final system configuration. The Agilent InfiniiVision DXO-X 2012A oscilloscope [13] is used again to determine the power delivered from the harvester, whose electro-mechanical configuration has been optimised as described in [14], to the load. As already explained above, power is determined by measuring the voltage on a known resistance (10 and 22 Ω), connected in series with the harvester and the sensor module. The thus obtained results are shown in Figure 10.

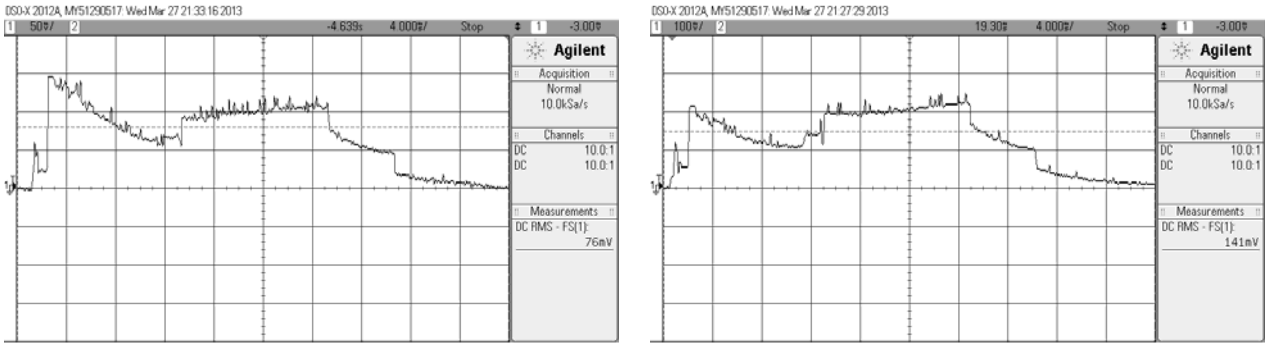

Figure 10. Measurement of the RMS voltage value on the resistor with R = 10 Ω (left) and with R = 22 Ω (right)

Considering the measured voltage V_{R_RMS} and using equation (1), the resulting average current I_{TPMS} will in this case be 7 mA. Using equation (4) it is thus possible to determine the power delivered to the load in the considered transmission time period as $P_{TPMS}(t_{TPMS}) \approx 23$ mW.

When the experimental results shown in Figure 10 are compared with those shown in Figure 8, it can be concluded that the voltage drop on the resistor is slightly higher when using the piezoelectric harvester, so that the average power delivered to the load is also slightly higher, while the transmission period lasts a little bit longer.

4.4 Laboratory experiments on final system configuration

In order to assess the validity of the thus developed optimised battery-less TPMS architecture, it is tested in laboratory conditions first. The respective experimental set-up is shown in Figure 11. It is based on a Schenk AG Vibroexciter 41 electrodynamics shaker with the corresponding signal generator and the Vibropower 41 power amplifier [15]. The coils in the exciter generate a dynamic excitation controllable in force units in a selectable frequency range (that can be swept) of up to 1 kHz. Tests are carried out with random vibrations so as to simulate the conditions that occur in real on-road conditions such as those described in section 2 of this work.

In the optimized configuration, the battery-less TPMS allowed tire pressure data to be successfully acquired and transmitted in average every 45 seconds. The effectiveness of the concept is thus successfully confirmed in laboratory conditions.

Figure 11. Experimental set-up: battery-less TPMS mounted on the shaker (left); excitation control unit (top right); oscilloscope used to monitor the system output (bottom right)

5. ON-ROAD EXPERIMENTS

Tests in real on-road conditions are carried on next. To mount the sensor module on a tire valve, a commercially available extension for the installation of the sensor on the valve is used (Figure 12). The extension is bonded with the module by using a two-component adhesive.

Figure 12. Extension of tire valve with sensor module

By mounting all the elements of the TPMS assembly on the tire rim (Figure 13), the electronics was successfully powered during the drive while acquiring pressure data and transmitting it to the receiver in the car cockpit thus proving effectively the proposed concept in real operating conditions.

Figure 13. Battery-less TPMS device mounted on the car tire rim

6. CONCLUSIONS AND OUTLOOK

In this work the electro mechanical design of a battery-less TPMS based on an energy harvesting device consisting of a bimorph piezoelectric cantilever is described. Laboratory experiments are performed first to determine the power consumption of the sensor. All elements of the battery-less TPMS are optimised next. Full functionality of the whole system is then proven in laboratory conditions. By designing suitable interfaces, the TPMS is finally mounted on a tire rim and successfully tested in real on-road settings. An extension of the concept towards a commercial solution that could be applied also in other fields is being pursued.

ACKNOWLEDGEMENTS

The work is supported through the “Ultra-high precision compliant devices for micro and nanotechnology applications” scientific project of the Croatian Ministry of Science, Education and Sports.

LIST OF SYMBOLS

CAP	internal rail referenced to V_{IN} to serve as the gate drive for the buck converter
C_{IN}	capacitance of the input capacitor
C_{OUT}	capacitance of the output capacitor
D_0, D_1	output voltage selection bits
GND	ground
I_{TPMS}	current in the circuit (delivered to the sensor electronics and transmitter)
L	inductance of the output inductor
$P_{LOAD}\,t_{LOAD}$	power requirements on the load for the desired duration

$P_{TPMS}(t_{TPMS})$	power delivered to the sensor electronics and transmitter in the transmission time period
P_{Z1}, P_{Z2}	connections for the piezoelectric harvester
R	resistance of the resistor mounted in series with the harvester and the sensor module
t_{LOAD}	desired duration of the output power
t_{TPMS}	transmission time period of the TPMS
v	vehicle speed
V_{IN}	rectified input voltage
V_{IN2}	internal low voltage rail to serve as the gate drive for the NMOS switch and as the logic high rail for the output voltage selection
V_{INMAX}	maximal value of the rectified input voltage
V_{INMIN}	minimal value of the rectified input voltage
V_{R_RMS}	voltage drop on the external resistor
V_{TPMS}	output voltage from the harvester and input voltage for the sensor module
$V_{UVLOFALLING}$	threshold undervoltage lockout voltage
η	average efficiency of the buck converter

REFERENCES

[1] Anton, S. R. and Sodano, H. A., “A review of power harvesting using piezoelectric materials,” Smart Mater. Struct. 16, 2-21 (2007).

[2] Kazmierski, T. J. and Beeby, S., [Energy harvesting systems: Principles, modelling and application], Springer (2011).

[3] Guyomar, D. and Lallart, M., “Recent progress in piezoelectric conversion and energy harvesting using nonlinear electronic interfaces and issues in small scale implementation,” Micromachines 2, 274-294 (2011).

[4] Lefeuvre, E., Lallart, M., Richard, C. and Guyomar, D., “Piezoelectric material-based energy harvesting devices: advances of SSH optimization techniques (1999-2009),” in Suaste-Gomez, E. (ed.), [Piezoelectric Ceramics], InTech Europe, 165-184 (2010).

[5] Roundy, S. J., “Energy scavenging for wireless sensor nodes with focus on a vibration to electricity conversion,” D. Sc. thesis, UC Berkeley (2003).

[6] Priya, Sh. and Inman, D. J. (ed.), [Energy Harvesting Technologies], Springer (2009).

[7] Álvarez, E. C. et al. (ed.), “Type approval requirements for the general safety of motor vehicles,” PE 408.573 EU Parliament (2008).

[8] Mide, Slam stick manual, 24 August 2010, rev. 001, <http://www.mide.com/pdfs/slamstick_datasheet.pdf>

[9] APC international Ltd., 16 November 2010, <http://www.americanpiezo.com/images/stories/content_images/pdf/APC_40-2010_20_30_40.pdf>

[10] Linear Technology, LTC3588-1 Piezoelectric energy harvesting power supply, September 2010, rev. A, <http://cds.linear.com/docs/en/datasheet/35881fa.pdf>

[11] FreeScale Semiconductor, Tire pressure monitor sensor product specification, May 2009, rev. 4, <http://www.freescale.com/files/sensors/doc/data_sheet/MPXY8300.pdf>

[12] Precision Engineering Laboratory, 2013, <http://precenglab.riteh.uniri.hr/?p=373>

[13] Agilent technologies, InfiniiVision 2000 X-series data sheet, 3 December 2012, <http://cp.literature.agilent.com/litweb/pdf/5990-6618EN.pdf>

[14] Zelenika, S. and Blažević, D., “Issues in validation of piezoelectric vibration-based energy harvesters,” Proc. SPIE 8066 806615-1 – 806615-11 (2011).

[15] Schenck, 2013, <http://schenck.net/en/>